Science of the Total Environment 857 (2023) 159624

Contents lists available at ScienceDirect

Science of the Total Environment

journal homepage: www.elsevier.com/locate/scitotenv

Marine plastics alter the organic matter composition of the air-sea boundary layer, with influences on CO_2 exchange: a large-scale analysis method to explore future ocean scenarios

Luisa Galgani [a,b,c,d,*], Eleni Tzempelikou [e], Ioanna Kalantzi [f], Anastasia Tsiola [f], Manolis Tsapakis [f], Paraskevi Pitta [f], Chiara Esposito [g], Anastasia Tsotskou [f,h], Iordanis Magiopoulos [f], Roberto Benavides [c], Tobias Steinhoff [c], Steven A. Loiselle [a,b,i]

[a] Environmental Spectroscopy Group, Department of Biotechnology, Chemistry and Pharmacy, University of Siena, Italy
[b] Center for Colloids and Surface Science, Sesto Fiorentino, Italy
[c] GEOMAR-Helmholtz Centre for Ocean Research Kiel, Germany
[d] Harbor Branch Oceanographic Institute, Florida Atlantic University, USA
[e] Institute of Oceanography, Hellenic Centre for Marine Research, Anavyssos, Greece
[f] Institute of Oceanography, Hellenic Centre for Marine Research, Heraklion, Greece
[g] Lake Ecology, Department of Ecoscience and WATEC Aarhus University Centre for Water Technology, Aarhus University, Denmark
[h] University of Western Macedonia, School of Agricultural Sciences, Department of Agriculture, Florina, Greece
[i] Consorzio Interuniversitario Nazionale per la Scienza e Tecnologia dei Materiali, Florence, Italy

HIGHLIGHTS

- A high plastic ocean in 3 m^3 mesocosms was simulated for the first time.
- Plastic enhances marine gels production and accumulation at the air-sea interface.
- Through marine gels accumulation, plastic alters the ocean-atmosphere gas exchange.
- High plastic amounts can affect the ocean's biological ability to mitigate climate.

GRAPHICAL ABSTRACT

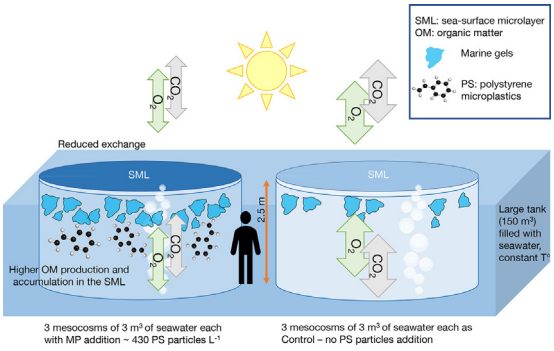

ARTICLE INFO

Editor: Damià Barceló

Keywords:
Microplastics
pCO_2
pH
Sea-surface microlayer
Mesocosms
Marine gel particles
Dissolved and particulate organic matter

ABSTRACT

Microplastics are substrates for microbial activity and can influence biomass production. This has potentially important implications in the sea-surface microlayer, the marine boundary layer that controls gas exchange with the atmosphere and where biologically produced organic compounds can accumulate. In the present study, we used six large scale mesocosms to simulate future ocean scenarios of high plastic concentration. Each mesocosm was filled with 3 m^3 of seawater from the oligotrophic Sea of Crete, in the Eastern Mediterranean Sea. A known amount of standard polystyrene microbeads of 30 μm diameter was added to three replicate mesocosms, while maintaining the remaining three as plastic-free controls. Over the course of a 12-day experiment, we explored microbial organic matter dynamics in the sea-surface microlayer in the presence and absence of microplastic contamination of the underlying water. Our study shows that microplastics increased both biomass production and enrichment of carbohydrate-like and proteinaceous marine gel compounds in the sea-surface microlayer. Importantly, this resulted in a ~3 % reduction in the

* Corresponding author at: Harbor Branch Oceanographic Institute of Florida Atlantic University, USA.
E-mail address: luisa.galgani@unisi.it (L. Galgani).

http://dx.doi.org/10.1016/j.scitotenv.2022.159624
Received 31 July 2022; Received in revised form 17 October 2022; Accepted 18 October 2022
Available online 21 October 2022

concentration of dissolved CO_2 in the underlying water. This reduction was associated to both direct and indirect impacts of microplastic pollution on the uptake of CO_2 within the marine carbon cycle, by modifying the biogenic composition of the sea's boundary layer with the atmosphere.

1. Introduction

The transition layer between environments is home to many fundamental physical, chemical and biological processes. The sea-surface microlayer (SML) is a millimetre-sized interface between the ocean and the atmosphere (Liss and Duce, 2005). It plays an essential role in ocean-climate feedbacks by mediating air-sea gas exchange and marine aerosol emission (Wurl et al., 2017). The SML has distinctly different biogeochemical properties with respect to its underlying seawater and it is enriched in both dissolved organic matter (DOM) and particulate organic matter (POM), in particular as carbohydrate-and protein-rich marine gel particles (Engel et al., 2017; Liss and Duce, 2005; Wurl and Holmes, 2008).

The two major classes of marine gel particles present in the SML are Transparent Exopolymer Particles (TEP) and Coomassie Stainable Particles (CSP). TEP and CSP give the SML its gel-like composition which is prevalent in most parts of the ocean (Wurl and Holmes, 2008) and support large and diversified microbial communities (Cunliffe and Murrell, 2009; Cunliffe et al., 2011), sensitive to local environmental and meteorological conditions (Rahlff et al., 2017; Zäncker et al., 2018). The enrichment of gel particles and their accompanying microbial life favours the creation of stable surface films that can influence the air-sea fluxes of oxygen and carbon dioxide (Calleja et al., 2013; Rahlff et al., 2019; Wurl et al., 2016).

Marine gel particles are derived from extracellular polymeric substances (EPS) released during microbial metabolic functions (Santschi et al., 2021). EPS exist in a continuum of sizes, including colloidal as well as dissolved and particulate fractions (Decho and Gutierrez, 2017; Verdugo, 2012). TEP and CSP are considered a class of EPS (Decho and Gutierrez, 2017) larger than 0.4 μm in relation to the pore size of the filter used for their analysis (Engel, 2009).

The microbial release of exopolymers is enhanced on plastic surfaces (Michels et al., 2018), part of the carbon-rich substrates that make up the resulting biofilm (Lear et al., 2021; Zhao et al., 2021). The presence of microplastics in natural and artificial seawater can stimulate the microbial release of DOM, probably due to a higher substrate availability for microbial growth (Boldrini et al., 2021; Galgani et al., 2018), as well as to carbon leachates from plastic that stimulate further microbial activity (Romera-Castillo et al., 2022a,b). Likewise, both nanoparticles and microparticles can induce EPS secretion by phytoplankton (Santschi et al., 2021; Shiu et al., 2020). The increased production of organic matter around plastic particles can promote biogenic aggregates formation (Shiu et al., 2020). These aggregates can move to the deep ocean (Galgani and Loiselle, 2021) or remain in the SML (Galgani and Loiselle, 2019).

As plastic particles sustain niches for high microbial activity (Amaral-Zettler et al., 2020; Zettler et al., 2013), one central hypothesis of the present study is that a higher concentration of microplastics in near surface conditions (<3 m depths) stimulates a higher microbial production of organic matter, adding on to the pool of organic compounds enriching the SML, and thereby modify the air-sea gas exchange properties of this interface.

It has been recently shown that seawater exposed plastic debris directly release climate relevant gases like DMS (Savoca et al., 2016), methane and ethylene (Royer et al., 2018), suggesting that significant concentrations of surface plastics may have a direct effect on water-air interactions. It has also been cited that important amounts of plastic can reduce the grazing pressure on phytoplankton in marine regions where nutrients are not a limiting factor, with subsequent anoxic conditions due to a cascade effect of initial high biomass production and degradation of the organic material (Kvale et al., 2021). Since much of the plastic at sea is concentrated in oligotrophic subtropical gyres (North Pacific, North Atlantic), it is expected that this additional carbon biomass on plastics offers a supplementary carbon source able to alter biogeochemical cycles (Zhao et al., 2021). Another key hypothesis of the present study is that high microplastic concentrations would promote high biomass production in oligotrophic conditions.

To test both hypotheses, pseudo-marine conditions needed to be created with well-defined and repeatable microplastic concentrations, but large enough to allow for particles aggregation, and for SML organic aggregates interaction with bulk water. Likewise, the experimental conditions should remain relatively stable over the medium term to allow for sampling of individual water masses with no mixing of waters with different microplastic concentrations. This was achieved by six large scale mesocosms, each filled with 3 m^3 of oligotrophic seawater from the oligotrophic Sea of Crete. Three of the mesocosms were amended with 30-μm diameter polystyrene microbeads (430 particles per L) and three were plastic-free control mesocosms (<0.5 particles larger than 1 μm per L). Prior to microplastic addition all mesocosms were controlled for uniformity. The SML and underlying water properties were subsequently compared over twelve days after the initial conditions.

2. Materials and methods

2.1. Mesocosms set up and SML sampling

Six mesocosms with a height of ~2.5 m and a diameter of 1.32 m made of transparent polyethylene (PE) were gravity-filled with 3 m^3 of coastal seawater pumped from below the surface (2 m) in the bay of Gournes (Sea of Crete). To ensure homogeneity of initial conditions, the water was divided equally in each of the six mesocosm and left overnight. The density of seawater during the experiment was 1.032 ± 0.001 g cm^{-3} with an average salinity of 41.4 ± 1.6 PSU. For the duration of the experiment (12 days), the mesocosms were kept in a 150 m^3 deep concrete tank with circulating seawater maintained at a constant temperature of 20 ± 1 °C. Each mesocosm was protected by a clear PVC lid to avoid atmospheric contamination. The first sampling (day 0) occurred the day after the mesocosms were filled. An aqueous solution of 30 μm diameter transparent polystyrene microbeads (Sigma-Aldrich, nr. 84,135) with a density of 1.05 g cm^{-3} was added to three mesocosms (MP1–3) after the first sampling (day 1) for a concentration of 430 microplastic L^{-1}, corresponding to about 5.92 μg C L^{-1}. The microparticles added were pure analytical standards: polystyrene spheres with a nominal diameter of 30 μm and a calibrated particle diameter of 30.94 ± 0.32 μm based on Coulter Multisizer III (Beckman) measurements provided by Sigma for batch BCBQ1422V (see Supplementary information). Polystyrene beads and polyethylene walls have a negative surface charge at pH above 2.5 (Beneš and Paulenová, 1973), reducing the possibility of attraction between the two materials in experimental conditions. We choose not to clean the mesocosms walls from any possible biofilm formation: we believe that this external procedure could significantly interfere with the parameters measured and be more invasive than the effect of periphyton biofilm formed in a few days, which experimental studies show being negligible for larger radius mesocosm (Chung-Chi and Kemp, 2004). Recent experiments show biofilm formation on PE films after extended incubation times (>60 and >90 days) (Gupta and Devi, 2020; Han et al., 2020), not comparable to the present experiment.

Each mesocosm was continuously gently mixed through a centralized airlift system situated just above the bottom surface to create a homogeneous distribution of the water, as described by Pitta et al. (2016). The mixing system was the same in each mesocosm. Mesocosm set up, manipulation, and sampling of the underlying water were conducted

daily (Galgani et al., 2019) according to standard methods for mesocosms studies performed at CretaCosmos facility (https://www.aquacosm.eu/mesocosm/cretacosmos/) (Pitta et al., 2016; Tsiola et al., 2017b). The sea-surface microlayer (SML) was sampled from each mesocosm early in the morning and prior to bulk water sampling every other day on day 0, day 1, day 3, day 5, day 7, day 9 and day 10, to allow a proper re-establishment of the surface film and minimise disturbance. The SML was sampled simultaneously in each mesocosm with 30 cm × 30 cm silicate glass plates with an effective sampling area of 1800 cm^2. Glass plates were inserted into the mesocosms perpendicular to the surface and withdrawn at a controlled rate of ~6 cm s^{-1} as suggested by Carlson (Carlson, 1982). The glass plate approach collects a thinner SML (~60–150 μm) when compared to, e.g., the Garrett screen (150–300 μm) (Garrett, 1965). The glass plate method allowed sampling of sufficient volume for analysis with a minimal dilution by the underlying water. The sample retained on both sides of the plate was removed with a wiper and poured into bottles with the aid of a funnel. The procedure was repeated until the necessary volume for analysis was obtained, tracking the exact number of dips per mesocosm. The first sample was discarded and used to rinse the collecting bottle. Glass plates, collecting bottles, wipers and funnels were acid cleaned (HCl 10 %) and Milli-Q rinsed prior use. To avoid cross-contamination, the control mesocosms and the microplastic-treated mesocosms had different sampling equipment (glass plates, funnels, collection bottles, wipers).

The thickness (d, μm) of the sampled SML was estimated as:

$$d = V/(A \times n) \quad (1)$$

where V is the SML volume collected, i.e., 60–140 mL, A is the sampling area of the glass plate (A = 1800 cm^2) and n is the number of dips. The apparent thickness of the SML ranged between 37 and 72 μm, with an overall mean of 54.7 ± 9.0 μm in agreement to previous studies (Carlson, 1982; Engel et al., 2018; Rahlff et al., 2019; Zäncker et al., 2017). The sampling thickness was similar for all mesocosms and sampling days. The samples were immediately processed in the laboratory within maximum 30 min after collection.

2.2. Dissolved Inorganic Carbon (DIC) and Total Alkalinity (TA) measurements

Following Dickson et al. (2007), seawater was drawn into 500 mL glass bottles using a tube to fill them from bottom to the top. Approximately half of the bottle volume was overflowed and a small headspace (approximately 1 % of the bottle volume) was left to allow for water expansion. The samples were fixed by adding 100 μL saturated mercury chloride ($HgCl_2$) solution thus preventing further biological activity, and stored in the dark at room temperature until analysis. The DIC measurements were performed using a coulometric technique with a SOMMA system (Johnson et al., 1998). The determination of TA was performed by potentiometric titration using a VINDTA system (Mintrop et al., 2000). Certified seawater samples were routinely measured to determine a precision estimated to 2.8 μmol kg^{-1} for DIC and 1.8 μmol kg^{-1} for TA.

2.3. Dissolved carbon dioxide estimates

The partial pressure of carbon dioxide in the mesocosms (pCO_2) as well as pH, CO_3^{2-}, HCO_3^- and CO_2 were calculated from DIC and TA at ambient temperature of 20 ± 1 °C and at sea-level pressure with the CO2SYS program (Pierrot et al., 2006) (https://cdiac.ess-dive.lbl.gov/ftp/co2sys/). We applied the equilibrium constants K1 and K2 of Lueker et al. (2000) as suggested by Dickson et al. (2007) and Orr et al. (2015) for a wider range of salinity and used a K_{SO4} value, the dissociation constant for HSO_4, of Dickson (1990).

2.4. Dissolved organic carbon (DOC) and chromophoric dissolved organic matter (CDOM)

Samples for DOC were filtered immediately after sampling in duplicate through 0.2 μm polycarbonate membranes and stored cool (+4 °C) in pre-combusted glass ampoules until analysis. Concentrations were determined using a Shimadzu TOC-V organic carbon analyser and following the high temperature catalytic oxidation method. The system was standardized prior to analysis using a potassium hydrogen phthalate standard solution. Each sample was injected 3 to 5 times and DOC concentrations were calculated from the average value of three replicates that yielded a relative standard deviation <2 %. Analytical precision and accuracy were tested against Deep Atlantic Seawater Reference Material provided by the DOC-CRM program (University of Miami – D.A. Hansell, batch 16); measured values: 0.510–0.580 (n = 10), certified value: 0.516–0.540. Drift correction of the DOC results was applied as needed.

Samples for CDOM were filtered immediately after collection in duplicates through 0.2 μm polyethersulfone syringe filters and stored cool (+4 °C) in pre-combusted amber glass vials until analysis, which was performed within 4 weeks. The CDOM absorbance spectrum was measured with a Lambda 10 ultraviolet-visible light (UV–Vis) Spectrophotometer (Perkin Elmer) from 210 to 750 nm at 960 nm/min, 1 nm wavelength resolution, and at room temperature (20 °C ± 2 °C). For each analysis, spectra were corrected for baseline, Milli-Q water absorbance and for scattering by subtracting the absorbance values at 730 nm. Absorption coefficients $a(\lambda)$ were calculated from absorbance values after Bricaud et al. (1981). The CDOM absorption spectral slope S (nm^{-1}) was determined by linear regression of log-transformed absorption spectra against the wavelength (Bricaud et al., 1981):

$$a(\lambda) = a_0 e^{-S(\lambda - \lambda_0)} \quad (2)$$

with $a(\lambda_0)$ being the absorption coefficient at a reference wavelength λ_0. We used multiple 20-nm wavelength intervals in a stepwise (1 nm) linear regression analysis according to Loiselle et al. (2009). Spectral slope correlates with changes in CDOM due to irradiation (photobleaching), and in the wavelength range 275–295, $S_{(275–295)}$ has been shown to be inversely related with DOM molecular weight (Helms et al., 2008).

2.5. Autotrophic and heterotrophic microorganisms

Abundances of autotrophic and heterotrophic microorganisms were measured by flow cytometry. Samples for heterotrophic bacteria were fixed with 25 % 0.2 μm-filtered glutaraldehyde (0.5 % final concentration), incubated at 4 °C for 45 min, flash frozen in liquid nitrogen and stored at −80 °C until analysis. Frozen samples were thawed at room temperature and sub-samples were stained for bacterial enumeration with the nucleic-acid stain SYBR Green I (final dilution 4 × 10^{-4} of the stock solution in Tris-EDTA buffer, pH = 8) and incubated for 10 min in the dark (Marie et al., 1997). The sample fluorescence signal was applied to distinguish high and low DNA content cells. Samples for autotrophic microorganisms were not fixed and were analysed without prior staining, based on their auto-fluorescence signal. A FACSCalibur™ flow cytometer (Becton Dickinson) was used following Tsiola et al. (2017a).

2.6. Marine gels

Total area and numbers of gel particles were determined by optical microscopy (Engel, 2009). Ten to fifteen milliliters of sample were filtered using 0.2 μm Nuclepore membranes (Whatman) and stained with 1 mL Alcian Blue solution for polysaccharidic gels (Transparent Exopolymer Particles, TEP) and 1 mL Coomassie Brilliant Blue G solution for proteinaceous gels (Coomassie Stainable Particles, CSP). Filters were mounted onto Cytoclear® slides and stored at −20 °C until microscopy analysis. For each slide, thirty images were taken randomly at 200× magnification with a light microscope equipped with a digital camera. The analysis of

the cross-sectional area of marine gels was performed with an image analysis software (ImageJ, U.S. National Institutes of Health) and used to calculate the equivalent spherical diameter (ESD) of individual particles, particles' number, volume and total area. The size frequency distribution of marine gel particles was determined according to their equivalent spherical diameter, described with a power function of the type:

$$\frac{dN}{d(d_p)} = k_p^{\delta} \quad (3)$$

with dN as the number of particles per unit volume in the size range d_p to $[d_p + d(d_p)]$, k a constant which depends on the concentrations of particles, and δ the slope ($\delta < 0$) describing the size distribution. A less negative δ implies an increase in the fraction of larger marine gels. k and δ were both derived from regressions of $\log[dN/d(d_p)]$ versus $\log[d_p]$ (Harlay et al., 2009; Mari and Burd, 1998; Mari and Kiørboe, 1996). The volume concentration of TEP and CSP refers to the mean volume of the particles >0.2 μm (membrane pore size cut-off); changes in this parameter indicate modifications in particle dynamics such as aggregation/disaggregation processes.

Since TEP are considered fractal aggregates, the volume and the carbon content of these marine gel particles are assumed to be proportional to r^D, with r being the equivalent spherical radius (μm) and D the fractal scaling dimension associated with the size-distribution of marine gels (Engel, 2009; Mari and Burd, 1998; Mari and Kiørboe, 1996). TEP carbon content (TEP—C, expressed in μg L^{-1}) was determined from marine gel size spectra according to Mari (1999) and Engel (2009):

$$\text{TEP} - \text{C}\ [\mu g\ L^{-1}] = 0.25 \times 10^{-6}\ r^D \quad (4)$$

with $D = -2.55$

2.7. Enrichment factors

To determine the enrichment or the depletion of each parameter analysed in the SML compared to the underlying water, we determined the Enrichment Factor (EF), defined as:

$$EF = \left([X]_\mu / [X]_b\right) \quad (5)$$

with $[X]_\mu$, $[X]_b$ the concentration of the specific parameter in the SML (μ) or underlying water (b) (Liss and Duce, 2005). An EF = 1 indicates that SML and underlying water values are similar, thus no significant enrichment or depletion in the SML can be observed. While bubbling may have promoted the enrichment of certain compounds in the SML, this process occurred in all mesocosms thus the influence of the airlift mixing system in the comparison of the dynamics of plastic free versus plastic enriched treatments is negligible.

2.8. Data analysis and statistics

To highlight the treatment effect (microplastics addition, MP mesocosms) and avoid the temporal variability, we calculated the normalized anomaly y_{ij} of each mesocosm (j) per day ($i = 0, \ldots, 11$) from the overall daily mean of the mesocosms $\overline{y}_i = \frac{1}{6}\sum_J^6 (x_j)_i$ following a procedure often applied in mesocosms studies (Endres et al., 2014; Engel et al., 2013):

$$y_{ij} = (x_{ij} - \overline{y}_i)/\overline{y}_i \quad (6)$$

Differences between control and treated mesocosms were determined by two-tailed unpaired *t*-tests and Mann-Whitney tests on normalized anomalies, depending on the distribution of the data. Repeated Measures Two-Way ANOVA and Mixed Effects Model (REML) were also used to analyse temporal variations between the control and microplastic treated mesocosms, the latter used in case of missing observations. This method is widely used to analyse data from mesocosms experiments (Dimitriou et al., 2017; Rahav et al., 2016). The fixed factor considered is the treatment (microplastics addition versus control) and the random effect is time (days). Correlations among parameters were determined by Multiple Linear Regression and Spearman correlation analysis. Statistical significance was accepted for $p < 0.05$ and considering a Bonferroni correction for multiple comparisons. All statistical tests were performed with Prism 8.02 (GraphPad Software, San Diego, CA, USA) and Minitab18 (Minitab Inc., USA).

3. Results

In an earlier study we reported an increase in the production of POM and marine gels in the bulk waters of the plastic-amended mesocosms with respect to the plastic-free controls (Galgani et al., 2019). In the present study, we explored differences in the composition of the SML and the possible influence of different SML compositions on the pCO_2 of the underlying bulk water. The SML was analysed for marine gel particles (TEP and CSP), autotrophic and heterotrophic microbial organisms, and dissolved organic matter parameters: Dissolved Organic Carbon, DOC, Chromophoric Dissolved Organic Matter, CDOM, and spectral slope, $S_{275\text{-}295}$. Salinity, total alkalinity and dissolved inorganic carbon (DIC) were measured from the underlying water and *in situ* pCO_2, pH, CO_3^{2-}, HCO_3^- and CO_2 were retrieved accordingly. All parameters described in the following paragraphs refer to the SML, except where specified. Biogeochemical processes and relevant data of the underlying water are described in a previous publication (Galgani et al., 2019) and were not the focus of this study.

3.1. Sea surface microlayer dynamics and underlying water pCO_2

Microplastic-amended mesocosms (MP) had significantly lower values of pCO_2 in the underlying water and higher pH compared to control mesocosms (Fig. 1). Mean values of pCO_2 in the MP treatments were almost 3 % lower than those found in control mesocosms, corresponding to an increase of 0.14 % in pH units (Table 1). Total alkalinity (TA) and dissolved inorganic carbon (DIC) were also significantly higher in the underlying water of MP treatments (Figs. 2 and S1). Similar differences were found for estimated concentrations of CO_3^{2-} and CO_2, with higher CO_3^{2-} in MP treatments (Fig. 2).

Higher concentrations of both polysaccharidic TEP and proteinaceous CSP were measured in the SML of the MP treated mesocosms (Fig. 1, Table 1). A 30 % increase in TEP and relative carbon content (TEP—C) along with higher concentrations and particle abundances of both marine gels occurred in the SML of the MP mesocosms, with a mean ± SEM (standard error of means) TEP-C of 424.8 ± 58.5 μg C L^{-1} compared to 324.3 ± 42.9 μg C L^{-1} in control mesocosms (Fig. 1). This was accompanied by a 1.4 % increase in *Synechococcus*, and by a 23.5 % increase of high-DNA containing *Synechococcus* cells in the SML (Figs. 1 and S2, Table 1), likely to be the main source of TEP for the whole system. In the underlying water of the mesocosms, an initial (and rapidly declined) phytoplankton bloom was attributed to the presence of autotrophic picoeukaryotes, while *Synechococcus* growth showed a constant increase and represented the dominant species in the mesocosms. This was expected as this species dominates in the oligotrophic waters of the Sea of Crete at this time of the year (Galgani et al., 2019). Heterotrophic bacteria concentrations in the SML were similar in MP and control mesocosms, and significant differences were observed over time rather than across treatments (Fig. S2, Table 1). Their concentrations were negatively correlated to those of *Synechococcus*, indicating a potential competition within the highly dynamic environment of the SML (Spearman $r = -0.40$, $p = 0.015$, $n = 37$). Alternating influence of primary and secondary production in the SML was also evidenced in the dynamics of the spectral slope $S_{275-295}$ of the chromophoric dissolved organic matter (CDOM) pool. Higher $S_{275-295}$ is associated to lower molecular weight CDOM often resulting from degradation processes, while lower $S_{275-295}$ characterises the "fresh" production of higher molecular weight CDOM (Helms et al., 2008).

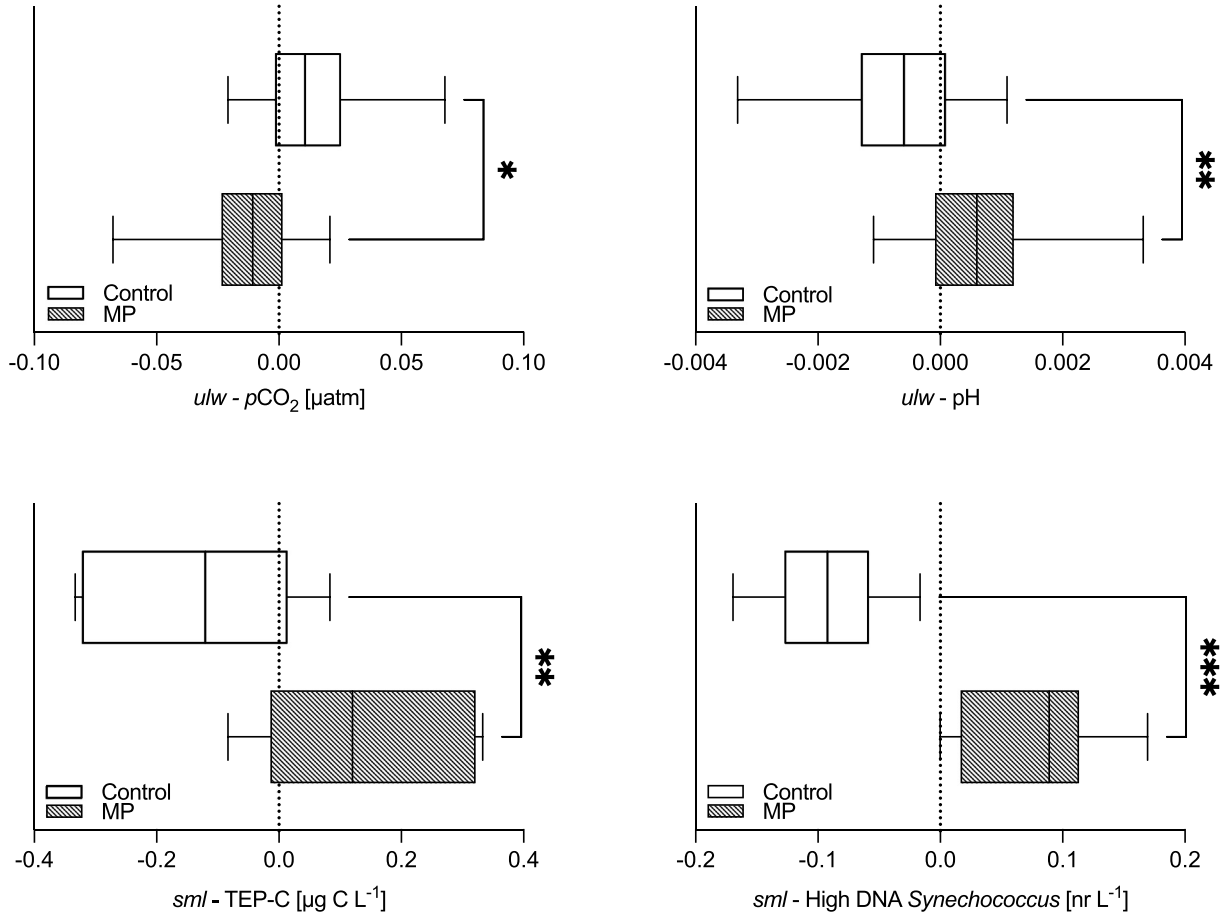

Fig. 1. Boxplots represent normalized anomalies and 5–95 percentiles for underlying water (ulw) pCO_2, pH, and for sea-surface microlayer (SML) Carbon contained in Transparent Exopolymer Particles (TEP—C) and High DNA containing *Synechococcus* cells. Stars indicate the level of significance in the differences between control and MP mesocosms based on Mann-Whitney tests on normalized anomalies (pCO_2, pH), and unpaired *t*-tests (TEP-C and High DNA *Synechococcus* cells).

While DOC and CDOM measured as the absorption coefficient at 355 nm ($a(355)$) were similar between control and MP mesocosms and significant variations were observed over time (Table 1, Fig. S3), $S_{275-295}$ instead was higher in the SML of MP mesocosms (Table 1, Fig. S3) confirming that there were significant differences in the DOM production and degradation processes between MP and Control treatments. In the SML, we observed a strong negative correlation between *Synechococcus* and $S_{275-295}$ (Table 2) as to indicate a release of organic matter from *Synechococcus* cells, and a weaker positive correlation between heterotrophic bacteria and $S_{275-295,}$ suggesting a bacterial degradation of organic compounds. $S_{275-295}$ was positively correlated to CSP ($mm^2\ L^{-1}$), DOC, and pCO_2 (Table 2) hinting to different production dynamics of CSP with respect to TEP and linking CSP concentration to organic matter degradation. In the SML, the amount of TEP-C was weakly related to the abundance of *Synechococcus* (Linear Regression $R^2 = 0.12$, $p = 0.03$) pointing to a local source (i.e., within the SML) of fresh biological production for this class of marine gel compounds. A positive correlation between DOC and $S_{275-295}$ suggested that the pool of DOC in the SML of the mesocosms was mostly composed of degraded or reworked material, and unlikely linked to a fresh biomass production.

Most importantly, we observed significant correlations between the pCO_2 in the underlying water (as well as pH, TA, DIC, CO_3^{2-} and CO_2) with the concentration of TEP-C and *Synechococcus* cells in the SML (Table 3). pCO_2 decreased with increasing TEP concentration and carbon content (Figs. 3 and S4a). Instead, CSP in the SML had the opposite relationship with pCO_2 with respect to TEP (Fig. 3). This was further demonstrated in the linear relationship between pCO_2 and marine gels concentrations (Eq. (7)):

$$pCO_2\ [\mu atm] = 413.189 - 0.0509\ TEP\ \left[mm^2\ L^{-1}\right] + 0.04708\ CSP\ \left[mm^2\ L^{-1}\right] \quad (7)$$

$R^2 = 0.38$, $p < 0.001$, $F = 11.98$

It should be noted that underlying water TEP and CSP concentrations from the same experiment did not show any relation to pCO_2. Together with SML gel concentrations, pCO_2 in the underlying water was related to SML $S_{275-295}$ and SML *Synechococcus* abundance (Figs. S4b, S4c and Tables 2 and 3), indicating the relationship of pCO_2 to different phases of organic matter cycling in the SML.

3.2. Sea surface microlayer enrichment and relation to underlying water parameters

In this experiment, the SML represented an enriched environment with respect to the underlying water conditions (Fig. 4). *Synechococcus* in the SML was strongly related to the underlying water cell abundances (Spearman $r = 0.945$, $p < 0.0001$, $n = 39$), as well as the amount of CDOM (Spearman $r = 0.859$, $p < 0.0001$, $n = 42$), the latter pointing to similar dynamics in DOM turnover between SML and underlying water. TEP concentration ($mm^2\ L^{-1}$) in the SML also showed a low but significant relation to underlying water TEP to some extent (Spearman $r = 0.359$, $p = 0.0197$, $n = 42$), confirming that most of the TEP variability in the SML was

Table 1
Repeated Measures Two-Way ANOVA or Mixed effects Model (REML) analysis table where the fixed factor is the "treatment" (MP/no MP) and the random effect is the time. Results are shown as the interaction of "treatment × time" unless otherwise noted. In bold: significant differences ($p < 0.05$) between MP mesocosms and Control mesocosms. Replicates within the treatments have been assumed having equal variability of differences. (*) and italics in columns "ANOVA F", "p value" and "Test" indicate differences that have been observed between MP and Control in time, and not as result of the interaction "treatment × time". Significant differences are accepted for $p < 0.05$.

Parameter/unit	ANOVA F	p value	Test	Mean control	Mean MP	SE of difference	% of difference MP/C
TA (ULW) [µmol kg^{-1}]	F (11, 43) = 3.138	**0.0035**	REML	2625.0	2631.0	1.77	0.2
DIC (ULW)* [µmol kg^{-1}]	*F (11, 43) = 9.482*	***<0.0001***	*REML (time)*	2283.0	2286.0	0.94	0.1
pCO_2 (ULW) [µatm]	F (11, 43) = 4.279	**0.0003**	REML	420.20	409.10	3.78	−2.6
pH (ULW)	F (11, 43) = 4.552	**0.0001**	REML	8.064	8.075	0.00	0.14
CO_3^{2-} (ULW) [µmol kg^{-1}]	F (11, 43) = 2.814	**0.0075**	REML	243.10	246.20	1.09	1.3
CO_2 (ULW) [µmol kg^{-1}]	F (11, 43) = 3.845	**0.0007**	REML	13.09	12.78	0.11	−2.4
HCO_3^- (ULW)* [µmol kg^{-1}]	*F (11, 43) = 2.991*	***0.0049***	*REML (time)*	2027.0	2027.0	1.27	0.0
TEP (SML)* [10^6 mm^2 L^{-1}]	*F (6, 24) = 3.573*	***0.0113***	*RM ANOVA (time)*	493.50	641.70	60.30	30.0
TEP (SML) [10^6 particles L^{-1}]	F (6, 24) = 2.836	**0.0312**	RM ANOVA	61.06	77.44	5.53	26.8
TEP-C (SML)* [µg Carbon L^{-1}]	*F (6, 24) = 3.868*	***0.0077***	*RM ANOVA (time)*	324.30	424.80	49.43	31.0
CSP (SML) [10^6 mm^2 L^{-1}]	F (6, 24) = 4.932	**0.002**	RM ANOVA	682.30	854.50	55.72	25.2
CSP (SML) [10^6 particles L^{-1}]	F (6, 24) = 4.870	**0.0022**	RM ANOVA	75.93	113.57	8.24	49.6
Syn (SML) [10^6 cells L^{-1}]	F (5, 20) = 4.417	**0.0071**	RM ANOVA	64.28	65.15	3.01	1.4
HDNA-Syn (SML)* [10^6 cells L^{-1}]	*F (5, 20) = 21.54*	***<0.0001***	*RM ANOVA (time)*	1.46	1.81	0.22	23.5
LDNA-Syn (SML) [10^6 cells L^{-1}]	F (5, 20) = 4.947	**0.0041**	RM ANOVA	62.85	63.35	2.84	0.8
$S_{275–295}$ (SML) [nm^{-1}]	F (6, 24) = 3.146	**0.0203**	RM ANOVA	0.01	0.01	0.00	4.1
a(355) nm (SML) [m^{-1}]	F (6, 24) = 1.090	0.3963	RM ANOVA	3.89	3.90	0.05	0.1
DOC (SML) [mg L^{-1}]	F (1, 4) = 0.02581	0.6927	REML	1.23	1.21	0.11	−1.5
H. Bacteria (SML)* [10^8 cells L^{-1}]	*F (6, 21) = 9.815*	***<0.0001***	*REML (time)*	4.46	4.31	0.42	−3.4
HDNA H. Bacteria (SML)* [10^8 cells L^{-1}]	*F (6, 21) = 10.40*	***<0.0001***	*REML (time)*	3.13	2.98	0.39	−4.8
LDNA H. Bacteria (SML)* [10^8 cells L^{-1}]	*F (6, 21) = 13.07*	***<0.0001***	*REML (time)*	1.27	1.34	0.05	5.3

SML = sea-surface microlayer; ULW = underlying water; TA = Total Alkalinity; DIC = Dissolved Inorganic Carbon; TEP = Transparent Exopolymer Particles; TEP-C = Carbon contained in Transparent Exopolymer Particles; CSP = Coomassie Stainable Particles; Syn = *Synechococcus* cells; HDNA-Syn = high DNA containing *Synechococcus* cells; LDNA-Syn = low DNA containing *Synechococcus* cells; $S_{275–295}$ = Spectral Slope measured between 275 and 295 nm; a(355) = CDOM (Chromophoric Dissolved Organic Matter) absorption coefficient at 355 nm; DOC = Dissolved organic Carbon; H. Bacteria = Heterotrophic Bacteria; HDNA H. Bacteria = high DNA containing heterotrophic bacterial cells; LDNA H. Bacteria = low DNA containing heterotrophic bacterial cells.

probably associated to *Synechococcus* cell abundances rather than to the underlying water TEP concentration.

Particularly high enrichment factors were observed for marine gels in the SML of all mesocosms, as expected. However, the enrichment factors for TEP and CSP were significantly higher in the MP mesocosms with respect to plastic-free controls (Fig. 5, Table S1) indicating that the SML of the mesocosms where plastic was added had a higher accumulation of marine gels (TEP and CSP).

4. Discussion

The twelve-day experiment coincided with a *Synechococcus* bloom phase in all six mesocosms, during which autotrophic production of particulate organic matter prevailed over heterotrophic activity. In the MP mesocosms there was an increased abundance of *Synechococcus* in the underlying water, which dominated over autotrophic picoeukaryotes cell numbers by an order of magnitude (Galgani et al., 2019). Microbial attachment on particles is a common phenomenon in aquatic ecosystems (Paerl, 1975) and microplastics may serve as a physical support for different microorganisms (Zettler et al., 2013; Zhao et al., 2021) creating hot spots of high metabolic activity (Dang and Lovell, 2015).

Synechococcus is an important primary producer in the Sea of Crete and a known TEP producer also in nutrient-limiting conditions (Deng et al., 2016; Ortega-Retuerta et al., 2019). Globally, *Synechococcus* contributes to 21 % of total CO_2 fixation (Jardillier et al., 2010).

We hypothesize that two concurrent processes led to the increased accumulation of TEP in the sea-surface microlayer of the mesocosms containing microplastics. Firstly, in the MP mesocosms, an increase in *Synechococcus* production led to higher TEP accumulation in the underlying water and enrichment in the SML possibly by migration of these compounds to the surface. The relationship between underlying water and SML marine gel particles is not novel in field (Engel and Galgani, 2016) and mesocosms studies (Galgani et al., 2014), since the SML partly reflects the underlying water composition. Secondly, *Synechococcus* cells can produce TEP directly in the SML (Yue et al., 2018) and their increased concentration in the SML of the MP mesocosms might have been an additional source for TEP accumulation.

In the ocean, TEP aggregation is proved to be a sink for marine carbon (Engel et al., 2004) and natural plankton communities are stimulated to

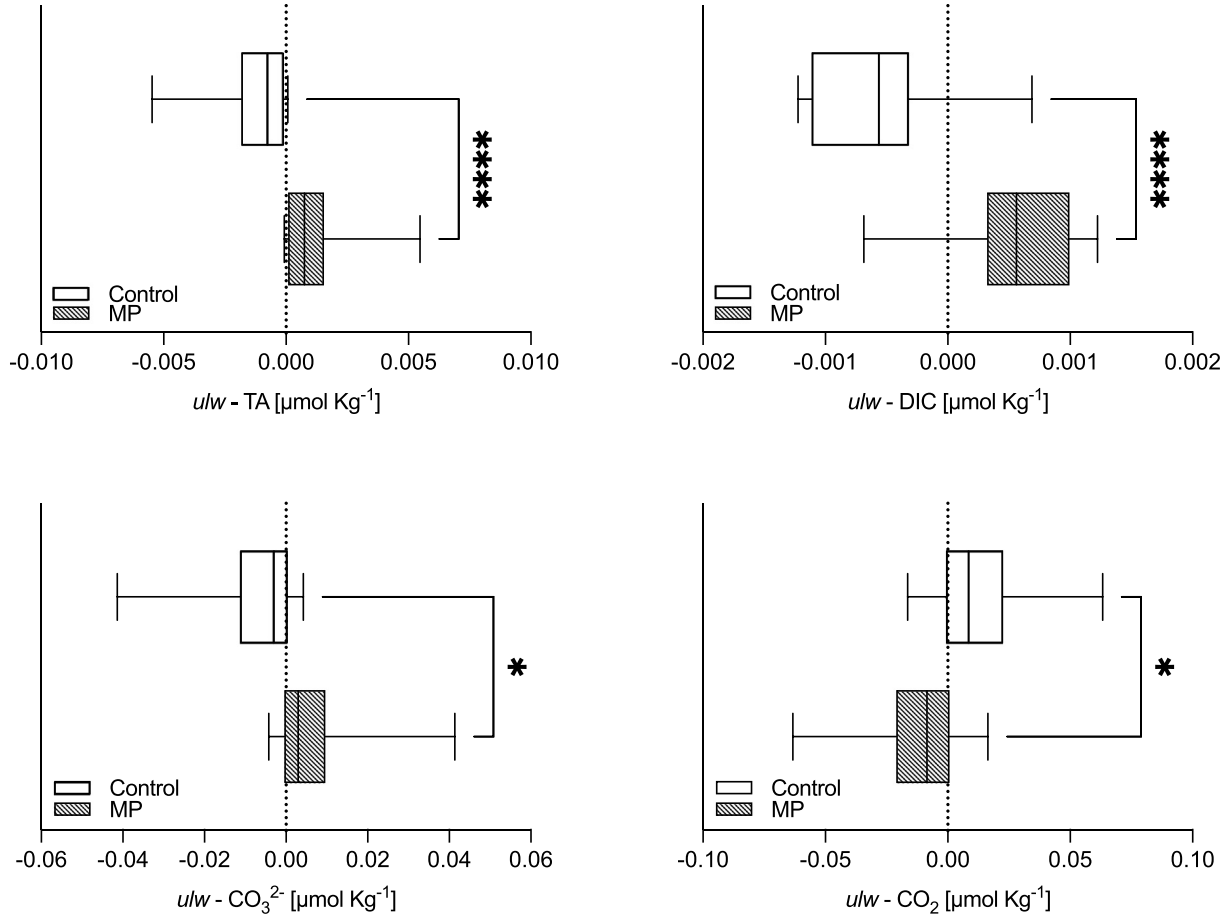

Fig. 2. Boxplots that represent normalized anomalies and 5–95 percentiles for underlying water (ulw) Total Alkalinity (TA), Dissolved Inorganic Carbon (DIC), CO_3^{2-} and CO_2. Stars indicate the level of significance in the differences between control and MP mesocosms based on Mann-Whitney test (TA, CO_3^{2-} and CO_2) and unpaired *t*-test (DIC).

produce TEP as a response to increased CO_2 (Engel, 2002). It has also been shown that microbial activity in the sea-surface microlayer can control the exchange rate of atmospheric CO_2 (Calleja et al., 2005); in our experiment, the higher TEP accumulation in the SML of the MP mesocosms may have served as a sink for CO_2 as described in Eq. (7).

To further support this difference, DIC partitioning in the underlying water of MP mesocosms had higher CO_3^{2-} and lower CO_2 concentrations with respect to plastic-free controls. This observation might be explained by the fact that *Synechococcus* has also been associated to "whiting" events in marine and lakes environments (Dittrich et al., 2003; Thompson et al.,

Table 2
Spearman r correlation table reporting significant correlations of Spectral Slope parameter in the SML (sea-surface microlayer) between 275 and 295 nm ($S_{275–295}$) to pCO_2 (ulw), and DOC, Heterotrophic Bacteria, CSP and *Synechococcus* cells in the SML. DOC = Dissolved organic Carbon; CSP = Coomassie Stainable Particles.

$S_{275–295}$ [nm^{-1}], SML	pCO_2 [µatm], ULW	DOC [mg L^{-1}], SML	Heterotrophic bacteria [cells L^{-1}], SML	CSP [mm^2 L^{-1}], SML	*Synechococcus* [cells L^{-1}], SML
Spearman r	0.51	0.45	0.34	0.35	−0.61
p	<0.001	0.004	0.032	0.024	<0.0001
n	42	39	39	42	39

Table 3
Spearman r correlation table between *Synechococcus* and Carbon contained in Transparent Exopolymer Particles (TEP—C) in the SML (sea-surface microlayer), to Total Alkalinity (TA), Dissolved Inorganic Carbon (DIC), pH, pCO_2 CO_3^{2-} and CO_2 in the underlying water of the mesocosms.

Synechococcus [cells L^{-1}]	TA [µmol kg^{-1}]	DIC [µmol kg^{-1}]	pH in	pCO_2 [µatm]	CO_3^{2-} [µmol kg^{-1}]	CO_2 [µmol kg^{-1}]
Spearman r	0.531	0.429	0.344	−0.33	0.336	−0.321
p	0.000557	0.00664	0.0323	0.0406	0.0368	0.0465
n	39	39	39	39	39	39

TEP-C [µg C L^{-1}]	TA [µmol kg^{-1}]	DIC [µmol kg^{-1}]	pH in	pCO_2 [µatm]	CO_3^{2-} [µmol kg^{-1}]	CO_2 [µmol kg^{-1}]
Spearman r	0.511	0.273	0.434	−0.433	0.481	−0.437
p	0.000592	0.0798	0.00428	0.00438	0.00137	0.00395
n	42	42	42	42	42	42

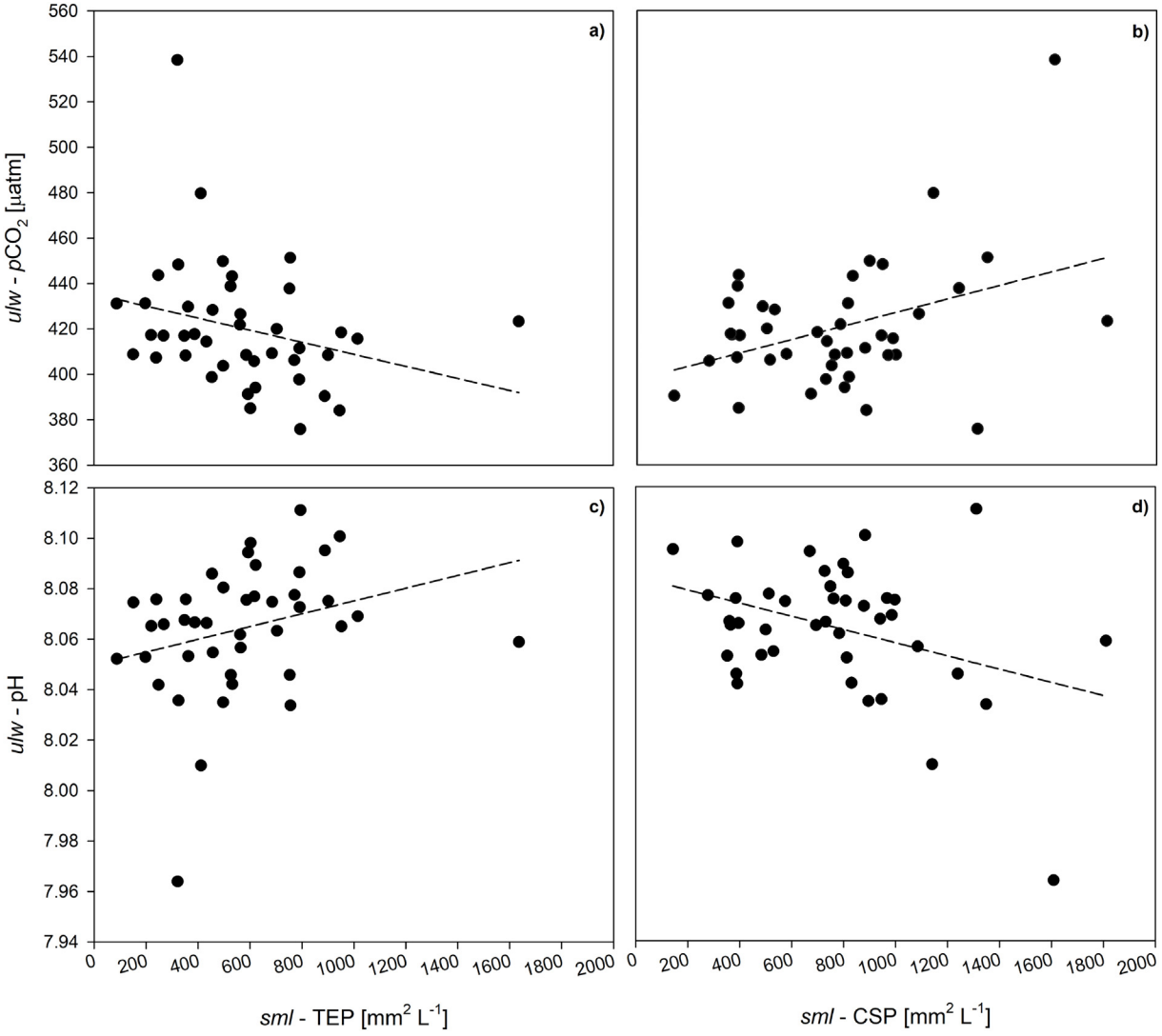

Fig. 3. Panels a, b: Multiple linear regression between pCO_2 in the underlying water (ulw) and the presence of marine gels (TEP, a; CSP, b) in the sea-surface microlayer (SML). Panels c, d: Multiple linear regression between pH in the underlying water (ulw) and marine gels (TEP, c; CSP, d) in the sea-surface microlayer (SML) according to the equation:
pH = 8.070 + 0.0000471 TEP [$mm^2\ L^{-1}$] − 0.0000421 CSP [$mm^2\ L^{-1}$].
For the regression, $R^2 = 0.365$, $p < 0.001$, F = 11.22, DF = 2. The panels have been displayed separately to better visualize the trends. TEP = Transparent Exopolymer Particles; CSP = Coomassie Stainable Particles.

1997). Whiting events occur when carbonates of biogenic origin are precipitated by microorganisms like cyanobacteria through photo-and chemosynthetic autotrophy in the presence of Mg(2+) and Ca(2+) counterions (Dittrich et al., 2003; Thompson, 2000; Thompson et al., 1997). Many bacteria species are implicated in $CaCO_3$ precipitation, which represents a potential mechanism for CO_2 sequestration and generally occurs at high pH, during active photosynthesis, and when DIC is limiting, such as after a bloom (Callieri, 2017). During the twelve-day experiment, the highest abundance of *Synechococcus* in the SML and underlying water appeared after the picoeukaryote and heterotrophic blooms (Galgani et al., 2019), corresponding to a migration and enrichment of organic compounds to the SML.

In particular, the enrichment of organic particles (i.e. TEP and CSP) in the SML of MP mesocosms led to the establishment of a highly enriched surface film, potentially able to modify gas exchange between the mesocosms and the surrounding atmosphere. The different partitioning of DIC between CO_3^{2-} and CO_2 in MP treatments confirms an increased autotrophy in MP mesocosms that led to lower pCO_2 beneath. In control mesocosms heterotrophy did not increase, rather, autotrophic production was less as additional substrates for microbial growth and metabolism, elsewhere provided by microplastics, were missing. This led to an overall lower production of marine gels in the underlying water and consequently in the SML, resulting in a less enriched surface film allowing for an increased exchange of atmospheric CO_2 at the air-sea interface. This is similar to the presence of surfactants in the sea-surface microlayer, where the resulting laminar diffusion layer reduces gas transfer (Frew, 1997). Some biogenic surfactants and surface slicks carrying a high microbial biomass can reduce air-sea CO_2 exchange by 15 % to 19 % (Mustaffa et al., 2020; Wurl et al., 2016).

While initially pCO_2 concentration might have been lower in the MP mesocosms, we should note that SML enrichment does not only limit the exchange of atmospheric CO_2, but also that of oxygen across the air-sea interface. In the post-bloom phase dominated by the heterotrophic remineralisation of organic matter, CO_2 is put back into the system through microbial respiration, while oxygen concentrations are reduced. The dynamics that we have observed in the mesocosms may be of high relevance in coastal, shallow and semi-enclosed marine areas affected by plastic and other types of organic or nutrient pollution that favour high

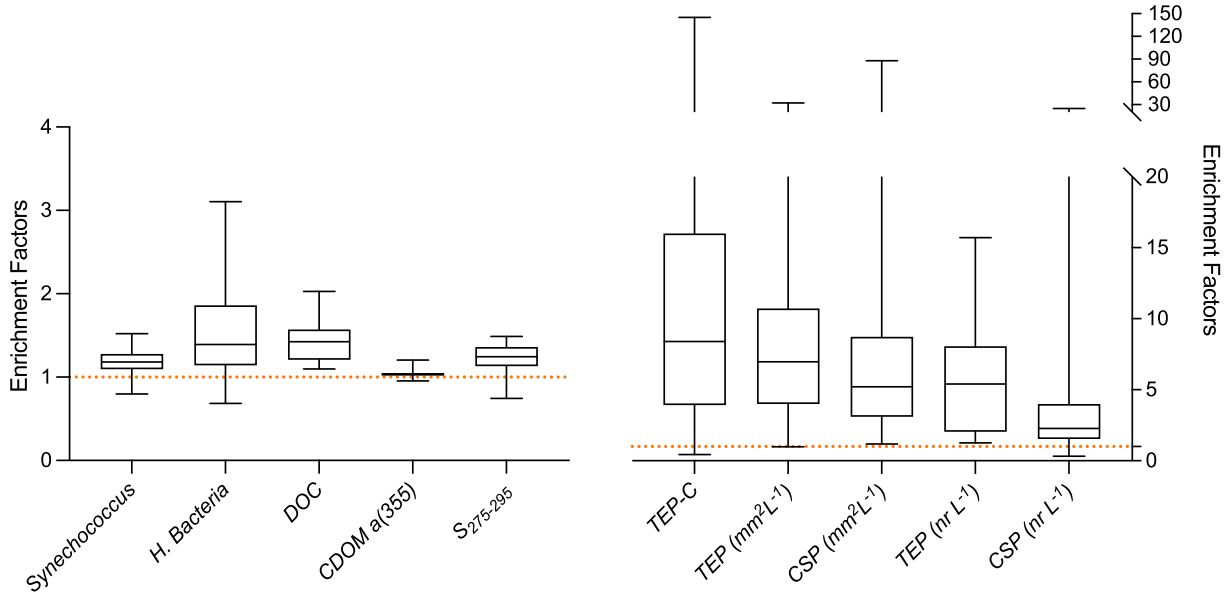

Fig. 4. Enrichment factors (EF) for sea-surface microlayer (SML) parameters compared to underlying water independently from the treatments (all data from control and MP mesocosms are merged). The dashed orange line is set on both graphs to EF = 1 which means no real differences between SML concentration and underlying water concentration. H. Bacteria = heterotrophic bacteria; DOC = Dissolved Organic Carbon; CDOM *a*(355) = Chromophoric Dissolved Organic Matter absorption coefficient at 355 nm; $S_{275–295}$ = Spectral Slope measured between 275 and 295 nm; TEP = Transparent Exopolymer Particles (as area and number); TEP-C = Carbon contained in Transparent Exopolymer Particles; CSP = Coomassie Stainable Particles (as area and number).

autotrophic biomass production. In areas where zooplankton feed on plastic particles because of high plastic concentration, grazing pressure on primary producers is reduced, further increasing autotrophic biomass in eutrophic waters, where the subsequent remineralisation of organic matter can further reduce oxygen concentrations (Kvale et al., 2021).

Our study shows that microplastics can increase the accumulation of marine gel particles in the SML by a 25–30 % compared to plastic-free conditions. By using large scale mesocosms, it was possible to explore daily changes in SML formation and the resulting impact on the underlying water pCO_2. This supports a better understanding of localized anoxic or hypoxic zones often observed in estuarine and upwelling areas where the SML plays an essential role in air-sea gas exchange (Engel and Galgani, 2016; Hepach et al., 2016; Upstill-Goddard, 2006) and where marine plastisphere communities can have direct effect on the concentration of N_2O and CO_2 (Cornejo-D'Ottone et al., 2020; Su et al., 2022).

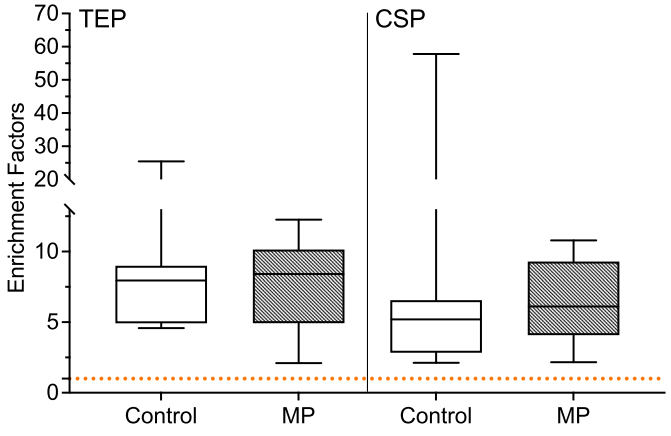

Fig. 5. Enrichment Factors (EFs) for the concentration of marine gels TEP and CSP, expressed as area $mm^2\ L^{-1}$, between Control and MP mesocosms. The orange dashed line indicates EF = 1. Repeated Measures two-way ANOVA tests (Table S1) have evidenced significant differences between EFs for marine gels. TEP = Transparent Exopolymer Particles; CSP = Coomassie Stainable Particles.

While this method demonstrated the indirect effect of plastics on seawater pCO_2 concentration through the SML, another effect that should be considered is the direct impact on the production and response of marine gels in the SML. TEP and CSP are distinct, insoluble macromolecules derived from the aggregation and annealing of DOM polymeric precursors produced during microbial growth and metabolism (Cisternas-Novoa et al., 2015; Engel, 2009; Thornton, 2018; Thornton et al., 2016). TEP concentrations in the SML were only partly related to those of the underlying water, indicating that an additional source of TEP may be the SML itself through the microbial activity of *Synechococcus*. As such, the SML may act as a direct sink of atmospheric CO_2 through extracellular polymers production within this layer. CSP instead seemed to be more clearly related to the degradation of organic matter present in the SML, as CDOM and $S_{275–295}$ measurements indicated their higher lability and rapid turnover (Thornton, 2018). This creates a pool of organic matter in the SML that is completely independent from underlying water processes, a phenomenon observed in highly productive marine regions (Galgani and Engel, 2016; Zäncker et al., 2017).

In the present study, we choose to use polystyrene as it is a very abundant microplastic polymer in oligotrophic marine areas (Pabortsava and Lampitt, 2020). While a recent study has reported that virgin laboratory grade polymer and commercially available polystyrene leaches dissolved organic carbon (DOC) in natural freshwater when exposed to dark and light conditions (Lee et al., 2020), such quantifiable DOC leachate was achieved at elevated concentrations of 5 $g\ L^{-1}$, or 10^6 times higher than the concentration used in the present study ($6 \times 10^{-6}\ g\ L^{-1}$).

The size of microplastics selected for use in the experiment allowed for the comparison to other studies on the influence of microplastics on marine biological processes like zooplankton ingestion (Cole et al., 2013, 2016) and human health (Hwang et al., 2020). Furthermore, the size range and concentration of the polystyrene particles were selected to minimise potential interference with spectrophotometric measurements of dissolved organic matter (Galgani et al., 2018), while allowing for them to be embedded into exopolymer gels in the field (Galgani et al., 2022).

It should be noted that the concentration of plastic particles used in this study was higher than typical marine conditions and more similar to those of impacted sediments in coastal areas (Sharma et al., 2021) and projections of future scenarios. While microplastics range between 1 μm and 5 mm (Andrady, 2011), most measurements of surface microplastics rely

on net tows with a limited mesh size, typically 330 μm (GESAMP, 2019). Therefore, microplastics smaller than 330 μm are largely under-sampled (Zhao et al., 2021), while being those most abundant, due to continuous plastic fragmentation processes. A recent study reported concentrations over ~8000 particles per L in the <333 μm size fraction (Brandon et al., 2020). Similarly, high concentrations of microplastics (10^5 particles m^{-3}) have been already found in a Swedish harbour in proximity of a plastic manufacture plant (Lindgren et al., 2016).

5. Conclusions

This mesocosm study shows an important new impact of plastic pollution on marine carbon biogeochemistry, that is the capacity of microplastics to directly influence processes at the air-sea boundary layer, in particular the ocean-atmosphere exchange of CO_2. Although not comparable to field observations, to the best of our knowledge, this experiment is the first to focus on the impacts of plastic on the sea-surface microlayer in a near natural setting, as *in situ* conditions of temperature, irradiation, and natural seawater biological and chemical composition were maintained.

Our results show that plastic pollution of the underlying water enhances the production and accumulation of two important classes of marine gels (polysaccharidic, TEP, versus proteinaceous, CSP) in the SML, with important repercussions on the control over the ocean's gas exchange with the atmosphere. Both indirect impacts, through an enriched surface film, as well as direct impacts, through an increase in the remineralisation of organic matter in the SML appear to be active. These results support the growing attention on the influence of plastic on the marine biological carbon pump and therefore on the ocean's capability to store anthropogenic CO_2 (Galgani and Loiselle, 2021; Kvale et al., 2021; Shen et al., 2020). Further efforts should be made to explore these dynamics across different marine environments and trophic regimes. Plastic production is expected to double in the next decades . In the absence of efficient management practices, plastic will continue to accumulate in our oceans and environment (Borrelle et al., 2020). Clearly, the impacts of plastic pollution on marine biogeochemistry go further than what explored in the present study. This highlights the importance of mesocosms-based studies and large-scale ocean simulations to better explore these dynamics, providing needed information to support international agreements to address climate change and the functionality of the oceanic carbon sink (Cooley et al., 2019).

CRediT authorship contribution statement

LG designed the experiment in consultation with SAL, MT and PP, analysed the data in consultation with SAL and wrote the manuscript. LG, ET, IK, AT, MT, PP, CE, ATso, IM, and SAL contributed to set up and experiment running, samples analysis and manuscript editing. RB and TS contributed to samples analysis and manuscript editing.

Data availability

All data will be made available on an open repository after publication in conformity with the requirements of all Horizon 2020 funded research projects.

Declaration of competing interest

The authors declare that they have no known competing financial interests or personal relationships that could have appeared to influence the work reported in this paper.

Acknowledgements

We greatly acknowledge G. Piperakis for the setting up of the mesocosms and for his technical assistance throughout the experiment. K. Mylona, I. Santi, S, Zivanovic, E. Dafnomili, S. Diliberto, and A. Loiselle are greatly acknowledged for technical support.

Funding

This work received funding from the European Union's Horizon 2020 Research and Innovation Programme under the Marie Skłodowska-Curie grant agreement No. 702747 – *POSEIDOMM*, to L. Galgani.

Appendix A. Supplementary data

Supplementary data to this article can be found online at https://doi.org/10.1016/j.scitotenv.2022.159624.

References

Amaral-Zettler, L.A., Zettler, E.R., Mincer, T.J., 2020. Ecology of the plastisphere. Nat. Rev. Microbiol. 18 (3), 139–151. https://doi.org/10.1038/s41579-019-0308-0.
Andrady, A.L., 2011. Microplastics in the marine environment. Mar. Pollut. Bull. 62 (8), 1596–1605. https://doi.org/10.1016/j.marpolbul.2011.05.030.
Beneš, P., Paulenová, M., 1973. Surface charge and adsorption properties of polyethylene in aqueous solutions of inorganic electrolytes. Kolloid Z. Z. Polym. 251 (10), 766–771. https://doi.org/10.1007/BF01499104.
Boldrini, A., Galgani, L., Consumi, M., Loiselle, S.A., 2021. Microplastics contamination versus inorganic particles: effects on the dynamics of marine dissolved organic matter. Environments 8 (3), 21. https://doi.org/10.3390/environments8030021.
Borrelle, Stephanie B., Ringma, Jeremy, Law, Kara Lavender, Monnahan, Cole C., Lebreton, Laurent, McGivern, Alexis, Murphy, Erin, Jambeck, Jenna, Leonard, George H., Hilleary, Michelle A., Eriksen, Marcus, Possingham, Hugh P., De Frond, Hannah, Gerber, Leah R., Polidoro, Beth, Tahir, Akbar, Bernard, Miranda, Mallos, Nicholas, Barnes, Megan, Rochman, Chelsea M., 2020. Predicted growth in plastic waste exceeds efforts to mitigate plastic pollution. Science 369 (6510), 1515–1518. https://doi.org/10.1126/science.aba3656.
Brandon, J.A., Freibott, A., Sala, L.M., 2020. Patterns of suspended and salp-ingested microplastic debris in the North Pacific investigated with epifluorescence microscopy. Limnol. Oceanogr. Lett. 5, 46–53. https://doi.org/10.1002/lol2.10127.
Bricaud, A., Morel, A., Prieur, L., 1981. Absorption by dissolved organic matter of the sea (yellow substance) in the UV and visible domains. Limnol. Oceanogr. 26, 43–53. https://doi.org/10.4319/lo.1981.26.1.0043.
Calleja, M.L., Duarte, C.M., Navarro, N., Agustí, S., 2005. Control of air-sea CO2 disequilibria in the subtropical NE Atlantic by planktonic metabolism under the ocean skin. Geophys. Res. Lett. 32 (8). https://doi.org/10.1029/2004GL022120.
Calleja, M.L., Duarte, C.M., Álvarez, M., Vaquer-Sunyer, R., Agustí, S., Herndl, G.J., 2013. Prevalence of strong vertical CO2 and O2 variability in the top meters of the ocean. Glob. Biogeochem. Cycles 27 (3), 941–949. https://doi.org/10.1002/gbc.20081.
Callieri, C., 2017. Synechococcus plasticity under environmental changes. FEMS Microbiol. Lett. 364 (23). https://doi.org/10.1093/femsle/fnx229.
Carlson, D.J., 1982. Phytoplankton in marine surface microlayers. Can. J. Microbiol. 28 (11), 1226–1234. https://doi.org/10.1139/m82-183.
Chung-Chi, C., Kemp, W.M., 2004. Periphyton communities in experimental marine ecosystems: scaling the effects of removal from container walls. Mar. Ecol. Prog. 271, 27–41. https://www.int-res.com/abstracts/meps/v271/p27-41/.
Cisternas-Novoa, C., Lee, C., Engel, A., 2015. Transparent exopolymer particles (TEP) and coomassie stainable particles (CSP): differences between their origin and vertical distributions in the ocean. Mar. Chem. 175, 56–71. https://doi.org/10.1016/j.marchem.2015.03.009.
Cole, M., Lindeque, P., Fileman, E., Halsband, C., Goodhead, R., Moger, J., Galloway, T.S., 2013. Microplastic ingestion by zooplankton. Environ. Sci. Technol. 47 (12), 6646–6655. https://doi.org/10.1021/es400663f.
Cole, M., Lindeque, P.K., Fileman, E., Clark, J., Lewis, C., Halsband, C., Galloway, T.S., 2016. Microplastics alter the properties and sinking rates of zooplankton faecal pellets. Environ. Sci. Technol. 50 (6), 3239–3246. https://doi.org/10.1021/acs.est.5b05905.
Cooley, S.R., Bello, B., Bodansky, D., Mansell, A., Merkl, A., Purvis, N., Ruffo, S., Taraska, G., Zivian, A., Leonard, G.H., 2019. Overlooked Ocean strategies to address climate change. Glob. Environ. Change 59, 101968. https://doi.org/10.1016/j.gloenvcha.2019.101968.
Cornejo-D'Ottone, M., Molina, V., Pavez, J., Silva, N., 2020. Greenhouse gas cycling by the plastisphere: the sleeper issue of plastic pollution. Chemosphere 246, 125709. https://doi.org/10.1016/j.chemosphere.2019.125709.
Cunliffe, M., Murrell, J.C., 2009. Eukarya 18S rRNA gene diversity in the sea surface microlayer: implications for the structure of the neustonic microbial loop. ISME J. 4 (3), 455–458. https://doi.org/10.1038/ismej.2009.133.
Cunliffe, M., Upstill-Goddard, R.C., Murrell, J.C., 2011. Microbiology of aquatic surface microlayers. FEMS Microbiol. Rev. 35 (2), 233–246. https://doi.org/10.1111/j.1574-6976.2010.00246.x.
Dang, H., Lovell, C.R., 2015. Microbial surface colonization and biofilm development in marine environments. Microbiol. Mol. Biol. Rev.: MMBR 80 (1), 91–138. https://doi.org/10.1128/MMBR.00037-15.
Decho, A.W., Gutierrez, T., 2017. Microbial extracellular polymeric substances (EPSs) in ocean systems. Front. Microbiol. 8. https://doi.org/10.3389/fmicb.2017.00922.
Deng, W., Cruz, B.N., Neuer, S., 2016. Effects of nutrient limitation on cell growth, TEP production and aggregate formation of marine synechococcus. Aquat. Microb. Ecol. 78 (1), 39–49. https://www.int-res.com/abstracts/ame/v78/n1/p39-49/.
Dickson, A.G., 1990. Standard potential of the reaction: AgCl(s) + 12H2(g) = Ag(s) + HCl (aq), and and the standard acidity constant of the ion HSO4− in synthetic sea water from 273.15 to 318.15 K. J. Chem. Thermodyn. 22 (2), 113–127. https://doi.org/10.1016/0021-9614(90)90074-Z.

Dickson, A.G., Sabine, C.L., Christian, J.R.E., 2007. Guide to best practices for ocean CO2 measurements. PICES special. Publication 3, 191 pp. https://www.ncei.noaa.gov/access/ocean-carbon-acidification-data-system/oceans/Handbook_2007.html.

Dimitriou, P.D., Papageorgiou, N., Geropoulos, A., Kalogeropoulou, V., Moraitis, M., Santi, I., Tsikopoulou, I., Pitta, P., Karakassis, I., 2017. A novel mesocosm setup for benthic-pelagic coupling experiments. Limnol. Oceanogr. Meth. 15 (4), 349–362. https://doi.org/10.1002/lom3.10163.

Dittrich, M., Müller, B., Mavrocordatos, D., Wehrli, B., 2003. Induced calcite precipitation by cyanobacterium synechococcus. Acta Hydrochim. Hydrobiol. 31 (2), 162–169. https://doi.org/10.1002/aheh.200300486.

Endres, S., Galgani, L., Riebesell, U., Schulz, K.-G., Engel, A., 2014. Stimulated bacterial growth under elevated pCO2: results from an off-shore mesocosm study. PLoS ONE 9 (6), e99228. https://doi.org/10.1371/journal.pone.0099228.

Engel, A., 2002. Direct relationship between CO2 uptake and transparent exopolymer particles production in natural phytoplankton. J. Plankton Res. 24 (1), 49–53. https://doi.org/10.1093/plankt/24.1.49.

Engel, A., 2009. Determination of marine gel particles. In: Wurl, O.E. (Ed.), Practical Guidelines for the Analysis of Seawater. CRC Press. https://doi.org/10.1201/9781420073072.ch7.

Engel, A., Galgani, L., 2016. The organic sea-surface microlayer in the upwelling region off the coast of Peru and potential implications for air–sea exchange processes. Biogeosciences 13 (4), 989–1007. https://doi.org/10.5194/bg-13-989-2016.

Engel, A., Thoms, S., Riebesell, U., Rochelle-Newall, E., Zondervan, I., 2004. Polysaccharide aggregation as a potential sink of marine dissolved organic carbon. Nature 428 (6986), 929–932. https://doi.org/10.1038/nature02453.

Engel, A., Borchard, C., Piontek, J., Schulz, K.G., Riebesell, U., Bellerby, R., 2013. CO2 increases 14C primary production in an Arctic plankton community. Biogeosciences 10 (3), 1291–1308. https://doi.org/10.5194/bg-10-1291-2013.

Engel, A., Bange, H.W., Cunliffe, M., Burrows, S.M., Friedrichs, G., Galgani, L., Herrmann, H., Hertkorn, N., Johnson, M., Liss, P.S., Quinn, P.K., Schartau, M., Soloviev, A., Stolle, C., Upstill-Goddard, R.C., van Pinxteren, M., Zäncker, B., 2017. The Ocean's vital skin: toward an integrated understanding of the sea surface microlayer. Front. Mar. Sci. 4 (165). https://doi.org/10.3389/fmars.2017.00165.

Engel, A., Sperling, M., Sun, C., Grosse, J., Friedrichs, G., 2018. Organic matter in the surface microlayer: insights from a wind Wave Channel experiment. Front. Mar. Sci. 5 (182). https://doi.org/10.3389/fmars.2018.00182.

Frew, N.M., 1997. The role of organic films in air–sea gas exchange. In: Liss, P.S., Duce, R.A. (Eds.), The Sea Surface and Global Change. Cambridge University Press, pp. 121–172. https://doi.org/10.1017/CBO9780511525025.006.

Galgani, L., Engel, A., 2016. Changes in optical characteristics of surface microlayers hint to photochemically and microbially mediated DOM turnover in the upwelling region off the coast of Peru. Biogeosciences 13 (8), 2453–2473. https://doi.org/10.5194/bg-13-2453-2016.

Galgani, L., Loiselle, S.A., 2019. Plastic accumulation in the sea surface microlayer: an experiment-based perspective for future studies. Geosciences 9. https://doi.org/10.3390/geosciences9020066.

Galgani, L., Loiselle, S.A., 2021. Plastic pollution impacts on marine carbon biogeochemistry. Environ. Pollut. 268, 115598. https://doi.org/10.1016/j.envpol.2020.115598.

Galgani, L., Stolle, C., Endres, S., Schulz, K.G., Engel, A., 2014. Effects of ocean acidification on the biogenic composition of the sea-surface microlayer: results from a mesocosm study. J. Geophys. Res. Oceans 119 (11), 7911–7924. https://doi.org/10.1002/2014jc010188.

Galgani, L., Engel, A., Rossi, C., Donati, A., Loiselle, S.A., 2018. Polystyrene microplastics increase microbial release of marine chromophoric dissolved organic matter in microcosm experiments. Sci. Rep. 8 (1), 14635. https://doi.org/10.1038/s41598-018-32805-4.

Galgani, L., Tsapakis, M., Pitta, P., Tsiola, A., Tzempelikou, E., Kalantzi, I., Esposito, C., Loiselle, A., Tsotskou, A., Zivanovic, S., Dafnomili, E., Diliberto, S., Mylona, K., Magiopoulos, I., Zeri, C., Pitta, E., Loiselle, S.A., 2019. Microplastics increase the marine production of particulate forms of organic matter. Environ. Res. Lett. https://doi.org/10.1088/1748-9326/ab59ca.

Galgani, L., Gossmann, I., Scholz-Böttcher, B., Jiang, X., Liu, Z., Scheidemann, L., Schlundt, C., Engel, A., 2022. Hitchhiking into the deep: how microplastic particles are exported through the biological carbon pump in the North Atlantic Ocean. Environ. Sci. Technol. https://doi.org/10.1021/acs.est.2c04712 (in press).

Garrett, W.D., 1965. Collection of slick-forming materials from the sea surface. Limnol. Oceanogr. 10, 602–605. https://doi.org/10.4319/lo.1965.10.4.0602.

GESAMP, 2019. Guidelines or the monitoring and assessment of plastic litter and microplastics in the ocean. In: Kershaw, P.J., Turra, A., Galgani, F. (Eds.), (IMO/FAO/UNESCO-IOC/UNIDO/WMO/IAEA/UN/UNEP/UNDP/ISA Joint Group of Experts on the Scientific Aspects of Marine Environmental Protection). Rep. Stud. GESAMP No. 99, p. 130.

Gupta, K.K., Devi, D., 2020. Characteristics investigation on biofilm formation and biodegradation activities of Pseudomonas aeruginosa strain ISJ14 colonizing low density polyethylene (LDPE) surface. Heliyon 6 (7), e04398. https://doi.org/10.1016/j.heliyon.2020.e04398.

Han, Y.N., Wei, M., Han, F., Fang, C., Wang, D., Zhong, Y.J., Guo, C.L., Shi, X.Y., Xie, Z.K., Li, F.M., 2020. Greater biofilm formation and increased biodegradation of polyethylene film by a microbial consortium of Arthrobacter sp. and Streptomyces sp. Microorganisms 8 (12). https://doi.org/10.3390/microorganisms8121979.

Harlay, J., De Bodt, C., Engel, A., Jansen, S., ÄôHoop, Q., Piontek, J., Van Oostende, N., Groom, S., Sabbe, K., Chou, L., 2009. Abundance and size distribution of transparent exopolymer particles (TEP) in a coccolithophorid bloom in the northern Bay of Biscay. Deep Sea Res. Part I Oceanogr. Res. Pap. 56 (8), 1251–1265. https://doi.org/10.1016/j.dsr.2009.01.014.

Helms, J.R., Stubbins, A., Ritchie, J.D., Minor, E.C., Kieber, D.J., Mopper, K., 2008. Absorption spectral slopes and slope ratios as indicators of molecular weight, source, and photobleaching of chromophoric dissolved organic matter. Limnol. Oceanogr. 53 (3), 955–969. https://doi.org/10.4319/lo.2008.53.3.0955.

Hepach, H., Quack, B., Tegtmeier, S., Engel, A., Bracher, A., Fuhlbrügge, S., Galgani, L., Atlas, E.L., Lampel, J., Frieß, U., Krüger, K., 2016. Biogenic halocarbons from the peruvian upwelling region as tropospheric halogen source. Atmos. Chem. Phys. 16 (18), 12219–12237. https://doi.org/10.5194/acp-16-12219-2016.

Hwang, J., Choi, D., Han, S., Jung, S.Y., Choi, J., Hong, J., 2020. Potential toxicity of polystyrene microplastic particles. Sci. Rep. 10 (1), 7391. https://doi.org/10.1038/s41598-020-64464-9.

Jardillier, L., Zubkov, M.V., Pearman, J., Scanlan, D.J., 2010. Significant CO2 fixation by small prymnesiophytes in the subtropical and tropical Northeast Atlantic Ocean. ISME J. 4 (9), 1180–1192. https://doi.org/10.1038/ismej.2010.36.

Johnson, K.M., Dickson, A.G., Eischeid, G., Goyet, C., Guenther, P., Key, R.M., Millero, F.J., Purkerson, D., Sabine, C.L., Schottle, R.G., Wallace, D.W.R., Wilke, R.J., Winn, C.D., 1998. Coulometric total carbon dioxide analysis for marine studies: assessment of the quality of total inorganic carbon measurements made during the US Indian Ocean CO2 survey 1994–1996. Mar. Chem. 63 (1), 21–37. https://doi.org/10.1016/S0304-4203(98)00048-6.

Kvale, K., Prowe, A.E.F., Chien, C.T., Landolfi, A., Oschlies, A., 2021. Zooplankton grazing of microplastic can accelerate global loss of ocean oxygen. Nat. Commun. 12 (1), 2358. https://doi.org/10.1038/s41467-021-22554-w.

Lear, G., Kingsbury, J.M., Franchini, S., Gambarini, V., Maday, S.D.M., Wallbank, J.A., Weaver, L., Pantos, O., 2021. Plastics and the microbiome: impacts and solutions. Environ. Microbiome 16 (1), 2. https://doi.org/10.1186/s40793-020-00371-w.

Lee, Y.K., Murphy, K.R., Hur, J., 2020. Fluorescence signatures of dissolved organic matter leached from microplastics: polymers and additives. Environ. Sci. Technol. 54 (19), 11905–11914. https://doi.org/10.1021/acs.est.0c00942.

Lindgren, J.F., Wilewska-Bien, M., Granhag, L., Andersson, K., Eriksson, K.M., 2016. Discharges to the sea. In: Andersson, K., Brynolf, S., Lindgren, J.F., Wilewska-Bien, M. (Eds.), Shipping and the Environment: Improving Environmental Performance in Marine Transportation. Springer, Berlin Heidelberg, pp. 125–168. https://doi.org/10.1007/978-3-662-49045-7_4.

Liss, P.S., Duce, R.A., 2005. The Sea Surface and Global Change. Cambridge University Press. https://doi.org/10.1017/CBO9780511525025.

Loiselle, S.A., Bracchini, L., Dattilo, A.M., Ricci, M., Tognazzi, A., Cózar, A., Rossi, C., 2009. The optical characterization of chromophoric dissolved organic matter using wavelength distribution of absorption spectral slopes. Limnol. Oceanogr. 54 (2), 590–597. https://doi.org/10.4319/lo.2009.54.2.0590.

Lueker, T.J., Dickson, A.G., Keeling, C.D., 2000. Ocean pCO2 calculated from dissolved inorganic carbon, alkalinity, and equations for K1 and K2: validation based on laboratory measurements of CO2 in gas and seawater at equilibrium. Mar. Chem. 70 (1), 105–119. https://doi.org/10.1016/S0304-4203(00)00022-0.

Mari, X., 1999. Carbon content and C: N ratio of transparent exopolymeric particles (TEP) produced by bubbling exudates of diatoms. Mar. Ecol. Prog. Ser. 183, 59–71. https://doi.org/10.3354/meps183059.

Mari, X., Burd, A., 1998. Seasonal size spectra of transparent exopolymeric particles (TEP) in a coastal sea and comparison with those predicted using coagulation theory. Mar. Ecol. Prog. Ser. 163, 63–76. https://doi.org/10.3354/meps163063.

Mari, X., Kiørboe, T., 1996. Abundance, size distribution and bacterial colonization of transparent exopolymeric particles (TEP) during spring in the Kattegat. J. Plankton Res. 18 (6), 969–986. https://doi.org/10.1093/plankt/18.6.969.

Marie, D., Partensky, F., Jacquet, S., Vaulot, D., 1997. Enumeration and cell cycle analysis of natural populations of marine picoplankton by flow cytometry using the nucleic acid stain SYBR green I. Appl. Environ. Microbiol. 63 (1), 186–193. https://doi.org/10.1128/aem.63.1.186-193.1997.

Michels, J., Stippkugel, A., Lenz, M., Wirtz, K., Engel, A., 2018. Rapid aggregation of biofilm-covered microplastics with marine biogenic particles. Proc. Royal Soc. B. https://doi.org/10.1098/rspb.2018.1203.

Mintrop, L., Pérez, F.F., González-Dávila, M., Santana-Casiano, J.M., Körtzinger, A., 2000. Alkalinity determination by potentiometry: intercalibration using three different methods. Cienc. Mar. 26 (1), 23–27. https://doi.org/10.7773/cm.v26i1.573.

Mustaffa, N.I.H., Ribas-Ribas, M., Banko-Kubis, H.M., Wurl, O., 2020. Global reduction of in situ CO2 transfer velocity by natural surfactants in the sea-surface microlayer. Proc. Math. Phys. Eng. Sci. 476 (2234), 20190763. https://doi.org/10.1098/rspa.2019.0763.

Orr, J.C., Epitalon, J.M., Gattuso, J.P., 2015. Comparison of ten packages that compute ocean carbonate chemistry. Biogeosciences 12 (5), 1483–1510. https://doi.org/10.5194/bg-12-1483-2015.

Ortega-Retuerta, E., Mazuecos, I.P., Reche, I., Gasol, J.M., Álvarez-Salgado, X.A., Álvarez, M., Montero, M.F., Arístegui, J., 2019. Transparent exopolymer particle (TEP) distribution and in situ prokaryotic generation across the deep Mediterranean Sea and nearby north East Atlantic Ocean. Prog. Oceanogr. 173, 180–191. https://doi.org/10.1016/j.pocean.2019.03.002.

Pabortsava, K., Lampitt, R.S., 2020. High concentrations of plastic hidden beneath the surface of the Atlantic Ocean. Nat. Comm. 11 (1), 4073. https://doi.org/10.1038/s41467-020-17932-9.

Paerl, H.W., 1975. Microbial attachment to particles in marine and freshwater ecosystems. Microb. Ecol. 2 (1), 73–83. https://doi.org/10.1007/bf02010382.

Pierrot, D., Lewis, E., Wallace, D.W.R., 2006. MS Excel Program Developed for CO2 System Calculations. ORNL/CDIAC-105a. Carbon Dioxide Information Analysis Center, Oak Ridge National Laboratory, U.S. Department of Energy, Oak Ridge, Tennessee. https://doi.org/10.3334/CDIAC/otg.CO2SYS_XLS_CDIAC105a.

Pitta, P., Nejstgaard, J.C., Tsagaraki, T.M., Zervoudaki, S., Egge, J.K., Frangoulis, C., Lagaria, A., Magiopoulos, I., Psarra, S., Sandaa, R.-A., Skjoldal, E.F., Tanaka, T., Thyrhaug, R., Thingstad, T.F., 2016. Confirming the "Rapid phosphorus transfer from microorganisms to mesozooplankton in the eastern Mediterranean Sea" scenario through a mesocosm experiment. J. Plankton Res. 38 (3), 502–521. https://doi.org/10.1093/plankt/fbw010.

Rahav, E., Shun-Yan, C., Cui, G., Liu, H., Tsagaraki, T.M., Giannakourou, A., Tsiola, A., Psarra, S., Lagaria, A., Mulholland, M.R., Stathopoulou, E., Paraskevi, P., Herut, B., Berman-Frank, I., 2016. Evaluating the impact of atmospheric depositions on springtime

dinitrogen fixation in the Cretan Sea (Eastern Mediterranean)—A mesocosm approach. Front. Mar. Sci. 3. https://doi.org/10.3389/fmars.2016.00180.
Rahlff, J., Stolle, C., Giebel, H.-A., Brinkhoff, T., Ribas-Ribas, M., Hodapp, D., Wurl, O., 2017. High wind speeds prevent formation of a distinct bacterioneuston community in the sea-surface microlayer. FEMS Microbiol. Ecol. 93 (5), fix041. https://doi.org/10.1093/femsec/fix041.
Rahlff, J., Stolle, C., Giebel, H.-A., Ribas-Ribas, M., Damgaard, L.R., Wurl, O., 2019. Oxygen profiles across the sea-surface microlayer—effects of diffusion and biological activity. Front. Mar. Sci. 6 (11). https://doi.org/10.3389/fmars.2019.00011.
Romera-Castillo, C., Birnstiel, S., Álvarez-Salgado, X.A., Sebastián, M., 2022. Aged plastic leaching of dissolved organic matter is two orders of magnitude higher than virgin plastic leading to a strong uplift in marine microbial activity. Front. Mar. Sci. 9, 861557. https://doi.org/10.3389/fmars.2022.861557.
Romera-Castillo, C., Mallenco-Fornies, R., Saá-Yánez, M., Álvarez-Salgado, X.A., 2022. Leaching and bioavailability of dissolved organic matter from petrol-based and biodegradable plastics. Mar. Environ. Res. 176, 105607. https://doi.org/10.1016/j.marenvres.2022.105607.
Royer, S.-J., Ferrón, S., Wilson, S.T., Karl, D.M., 2018. Production of methane and ethylene from plastic in the environment. PLoS ONE 13 (8), e0200574. https://doi.org/10.1371/journal.pone.0200574.
Santschi, P.H., Chin, W.-C., Quigg, A., Xu, C., Kamalanathan, M., Lin, P., Shiu, R.-F., 2021. Marine gel interactions with hydrophilic and hydrophobic pollutants. Gels 7 (3), 83. https://www.mdpi.com/2310-2861/7/3/83.
Savoca, M.S., Wohlfeil, M.E., Ebeler, S.E., Nevitt, G.A., 2016. Marine plastic debris emits a keystone infochemical for olfactory foraging seabirds. Sci. Adv. 2 (11), e1600395. https://doi.org/10.1126/sciadv.1600395.
Sharma, S., Sharma, V., Chatterjee, S., 2021. Microplastics in the Mediterranean Sea: sources, pollution intensity, sea health, and regulatory policies. Front. Mar. Sci. 8. https://doi.org/10.3389/fmars.2021.634934.
Shen, M., Ye, S., Zeng, G., Zhang, Y., Xing, L., Tang, W., Wen, X., Liu, S., 2020. Can microplastics pose a threat to ocean carbon sequestration? Mar. Pollut. Bull. 150, 110712. https://doi.org/10.1016/j.marpolbul.2019.110712.
Shiu, R.-F., Vazquez, C.I., Chiang, C.-Y., Chiu, M.-H., Chen, C.-S., Ni, C.-W., Gong, G.-C., Quigg, A., Santschi, P.H., Chin, W.-C., 2020. Nano- and microplastics trigger secretion of protein-rich extracellular polymeric substances from phytoplankton. Sci. Total Environ. 748, 141469. https://doi.org/10.1016/j.scitotenv.2020.141469.
Su, X., Yang, L., Yang, K., Tang, Y., Wen, T., Wang, Y., Rillig, M.C., Rohe, L., Pan, J., Li, H., Zhu, Y.-G., 2022. Estuarine plastisphere as an overlooked source of N2O production. Nat. Commun. 13 (1), 3884. https://doi.org/10.1038/s41467-022-31584-x.
Thompson, J.B., 2000. Microbial whitings. In: Riding, R.E., Awramik, S.M. (Eds.), Microbial Sediments. Springer, Berlin Heidelberg, pp. 250–260. https://doi.org/10.1007/978-3-662-04036-2_27.
Thompson, J.B., Schultze-Lam, S., Beveridge, T.J., Des Marais, D.J., 1997. Whiting events: biogenic origin due to the photosynthetic activity of cyanobacterial picoplankton. Limnol. Oceanogr. 42 (1), 133–141. https://doi.org/10.4319/lo.1997.42.1.0133.
Thornton, D.C.O., 2018. Coomassie stainable particles (CSP): protein containing exopolymer particles in the ocean. Front. Mar. Sci. 5 (206). https://doi.org/10.3389/fmars.2018.00206.
Thornton, D.C.O., Brooks, S.D., Chen, J., 2016. Protein and carbohydrate exopolymer particles in the sea surface microlayer (SML). Front. Mar. Sci. 3 (135). https://doi.org/10.3389/fmars.2016.00135.
Tsiola, A., Pitta, P., Callol, A.J., Kagiorgi, M., Kalantzi, I., Mylona, K., Santi, I., Toncelli, C., Pergantis, S., Tsapakis, M., 2017. The impact of silver nanoparticles on marine plankton dynamics: dependence on coating, size and concentration. Sci. Total Environ. 601–602, 1838–1848. https://doi.org/10.1016/j.scitotenv.2017.06.042.
Tsiola, A., Tsagaraki, T.M., Giannakourou, A., Nikolioudakis, N., Yücel, N., Herut, B., Pitta, P., 2017. Bacterial growth and mortality after deposition of saharan dust and mixed aerosols in the eastern Mediterranean Sea: a mesocosm experiment. Front. Mar. Sci. 3. https://doi.org/10.3389/fmars.2016.00281.
Upstill-Goddard, R.C., 2006. Air–sea gas exchange in the coastal zone. Estuar. Coast. Shelf Sci. 70 (3), 388–404. https://doi.org/10.1016/j.ecss.2006.05.043.
Verdugo, P., 2012. Marine microgels. Ann. Rev. Mar. Sci. 4 (1), 375–400. https://doi.org/10.1146/annurev-marine-120709-142759.
Wurl, O., Holmes, M., 2008. The gelatinous nature of the sea-surface microlayer. Mar. Chem. 110 (1–2), 89–97. https://doi.org/10.1016/j.marchem.2008.02.009.
Wurl, O., Stolle, C., Van Thuoc, C., The Thu, P., Mari, X., 2016. Biofilm-like properties of the sea surface and predicted effects on air–sea CO2 exchange. Prog. Oceanogr. 144, 15–24. https://doi.org/10.1016/j.pocean.2016.03.002.
Wurl, O., Ekau, W., Landing, W.M., Zappa, C.J., 2017. Sea surface microlayer in a changing ocean – a perspective. ElementaSci. Anthrop. 5 (31). https://doi.org/10.1525/elementa.228.
Yue, W.-z., Sun, C.-c., Shi, P., Engel, A., Wang, Y.-s., He, W.-H., 2018. Effect of temperature on the accumulation of marine biogenic gels in the surface microlayer near the outlet of nuclear power plants and adjacent areas in the Daya Bay, China. PLoS ONE 13 (6), e0198735. https://doi.org/10.1371/journal.pone.0198735.
Zäncker, B., Bracher, A., Röttgers, R., Engel, A., 2017. Variations of the organic matter composition in the sea surface microlayer: a comparison between Open Ocean, coastal, and upwelling sites off the Peruvian coast. Front. Microbiol. 8 (2369). https://doi.org/10.3389/fmicb.2017.02369.
Zäncker, B., Cunliffe, M., Engel, A., 2018. Bacterial community composition in the sea surface microlayer off the Peruvian coast. Front. Microbiol. 9 (2699). https://doi.org/10.3389/fmicb.2018.02699.
Zettler, E.R., Mincer, T.J., Amaral-Zettler, L.A., 2013. Life in the "Plastisphere": microbial communities on plastic marine debris. Environ. Sci. Technol. 47 (13), 7137–7146. https://doi.org/10.1021/es401288x.
Zhao, S., Zettler, E.R., Amaral-Zettler, L.A., Mincer, T.J., 2021. Microbial carrying capacity and carbon biomass of plastic marine debris. ISME J. 15 (1), 67–77. https://doi.org/10.1038/s41396-020-00756-2.